DOI: 10.24352/UB.OVGU-2019-021 TECHNISCHE MECHANIK, 39, 2, (2019), 229 – 240
submitted: November 29, 2018

Application of the Classical Beam Theory for Studying Lengthwise Fracture of Functionally Graded Beams

V. Rizov, H. Altenbach

The present paper deals with analysis of lengthwise cracks in linear-elastic functionally graded beam configurations. A general approach for deriving of the strain energy release rate is developed by applying the classical beam theory. A crack located arbitrary along the beam thickness is considered, i.e. the crack arms have different thicknesses. The approach holds for beams which are functionally graded in the thickness direction (the modulus of elasticity can be distributed arbitrary along the thickness of the beam). The approach is applied to analyze the strain energy release rate for a lengthwise crack in a functionally graded cantilever beam. The beam is loaded by one concentrated force applied at the free end of the upper crack arm. An exponential law is used to describe the continuous variation of the modulus of elasticity along the beam thickness. The solution to the strain energy release rate in the cantilever beam is verified by applying the J-integral approach. The solution is verified further by using the compliance method for deriving the strain energy release rate. The effects of crack location along the beam thickness, crack length and material gradient on the strain energy release rate in the functionally graded cantilever beam are analyzed by applying the solution derived.

1 Introduction

The quick development of engineering demands an extensive use of high performance structural materials such as functionally graded materials. The novel inhomogeneous composites known as functionally graded materials are composed of two or more constituent materials. The basic idea of the functionally graded materials is that by allowing a gradual variation of the composition of the constituent materials in one or more spatial directions, the material properties are modified to meet different material performance requirements in different parts of a structural member (Gasik, 2010; Jha *et al*., 2013; Knoppers *et al*., 2003; Mahamood and Akinlabi, 2017; Miyamoto *et al*., 1999; Nemat-Allal *et al*., 2011; Wu *et al*., 2014; Zhang *et al*., 2011). Thus, it is not surprising that application of functionally graded materials as advanced structural materials in the practical engineering has increased significantly for the last three decades.

Understanding the fracture behaviour is very important for the structural applications of functionally graded materials (Carpinteri and Pugno, 2006; Dolgov, 2005; Dolgov, 2016; Erdogan, 1995; Paulino, 2002; Rizov, 2017; Rizov, 2018; Tilbrook *et al*., 2005; Upadhyay and Simha, 2007; Uslu Uysal and Güven, 2016). The presence of cracks drastically reduces the load-bearing capacity of functionally graded structural members and components. Also, the structural integrity and reliability of functionally graded materials and structures essentially depend upon their fracture behaviour. Therefore, development of methods for fracture analyses is vital for evaluation of operational performance of functionally graded engineering structures.

The present paper aim is to develop an approach for analyzing the lengthwise fracture behaviour of functionally graded beams in terms of the strain energy release rate by applying the classical linear-elastic beam theory. Analyses of lengthwise fracture are needed since some functionally graded materials can be built-up layer by layer (Mahamood and Akinlabi, 2017) which is a premise for appearance of lengthwise cracks between layers. It should be mentioned that while the previous publications (Rizov, 2017; Rizov, 2018) are focussed on analyzing the strain energy release rate for lengthwise cracks in individual beam configurations, the present paper develops a general approach for the strain energy release rate. The beams under consideration are functionally graded in the thickness direction (it is assumed that the modulus of elasticity varies continuously along the beam thickness). The general approach developed is applicable for a lengthwise crack located arbitrary along the beam thickness.

Besides, the law that describes the distribution of the modulus of elasticity in the thickness direction is arbitrary. The approach is used to calculate the strain energy release rate for a functionally graded cantilever beam configuration containing a lengthwise crack. The *J*-integral method is applied to verify the solution to the strain energy release rates. The solution is verified also by using the compliance method. Parametric investigations are performed in order to evaluate the effects of various material and geometrical parameters on the lengthwise fracture behaviour.

2 Deriving of the Strain Energy Release Rate

A portion of a functionally graded beam containing a lengthwise crack is shown in Figure 1. The beam has a rectangular cross-section of width, b, and thickness, $2h$. The thicknesses of the lower and upper crack arms are denoted by h_1 and h_2, respectively.

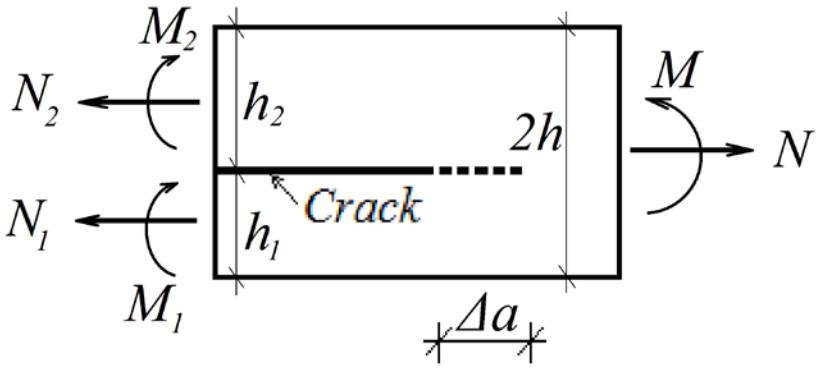

Figure 1. Portion of a functionally graded beam with a lengthwise crack (Δa is a small increase of the crack length, h_1 and h_2 are, respectively, the thicknesses of the lower and upper crack arms).

The bending moment and axial force in the beam cross-section ahead of the crack tip are denoted by M and N, respectively. In order to derive the strain energy release rate, G, a small increase, Δa, of the crack length is assumed. The strain energy release rate is written as

$$G = -\frac{\Delta U}{\Delta A}, \tag{1}$$

where ΔU is the change of the strain energy, ΔA is the increase of crack area. Since

$$\Delta A = b\Delta a, \tag{2}$$

formula (1) is re-written as

$$G = -\frac{\Delta U}{b\Delta a}. \tag{3}$$

The change of the strain energy is expressed as a difference between the strain energy cumulated in the beam portion of length, Δa, before the increase of crack and the strain energy cumulated in the portions of two crack arms of length, Δa, behind the crack tip

$$\Delta U = \Delta a\, b \int_{-h}^{h} u_{03} dz_3 - \Delta a\, b \int_{-\frac{h_1}{2}}^{\frac{h_1}{2}} u_{01} dz_1 - \Delta a\, b \int_{-\frac{h_2}{2}}^{\frac{h_2}{2}} u_{02} dz_2 \ , \tag{4}$$

where u_{01}, u_{02} and u_{03} are, respectively, the strain energy densities in the lower and upper crack arms and the un-cracked beam portion ahead of the crack tip, z_1, z_2 and z_3 are, respectively, the vertical centroidal axes of the cross-sections of lower and upper crack arms and the un-cracked beam portion. By combining of (3) and (4), one arrives at the following expression for the strain energy release rate:

$$G = \int_{-\frac{h_1}{2}}^{\frac{h_1}{2}} u_{01} dz_1 + \int_{-\frac{h_2}{2}}^{\frac{h_2}{2}} u_{02} dz_2 - \int_{-h}^{h} u_{03} dz_3 \ . \tag{5}$$

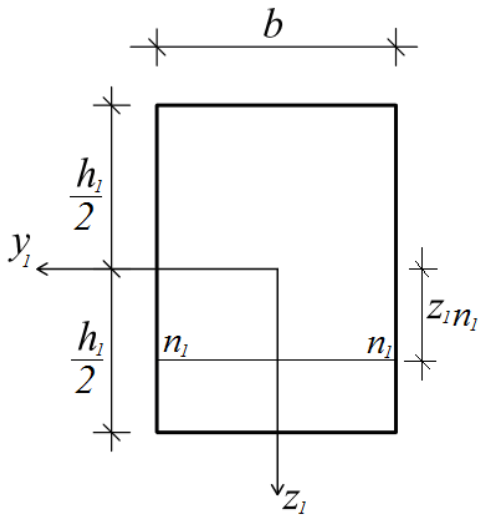

Figure 2. Cross-section of the lower crack arm ($n_1 - n_1$ is the position of the neutral axis).

The strain energy density in the cross-section of lower crack arm behind the crack tip is written as

$$u_{01} = \frac{1}{2}\sigma\varepsilon \,, \tag{6}$$

where σ is the normal stress, ε is the lengthwise strain. The normal stress is obtained by applying the Hooke's law

$$\sigma = E\varepsilon \,, \tag{7}$$

where the modulus of elasticity, E, is distributed continuously in the thickness direction

$$E = E\left(z_1\right). \tag{8}$$

Beams of high length to thickness ratio are considered in the present paper. Therefore, according to the Bernoulli's hypothesis for plane sections the lengthwise strain is distributed linearly along the thickness of the lower crack arm

$$\varepsilon = \kappa_1\left(z_1 - z_{1n_1}\right), \tag{9}$$

where κ_1 is the curvature of the lower crack arm, z_{1n_1} is the coordinate of the neutral axis (Figure 2). It should be mentioned that the neutral axis shifts from the centroid since the material is functionally graded in the thickness direction and, also, the beam is under combination of axial force and bending moment.

The curvature and the coordinate of the neutral axis of the lower crack arm are determined from the following equations for equilibrium of the cross-section:

$$N_1 = b\int_{-\frac{h_1}{2}}^{\frac{h_1}{2}} \sigma \, dz_1 , \tag{10}$$

$$M_1 = b\int_{-\frac{h_1}{2}}^{\frac{h_1}{2}} \sigma \, z_1 dz_1 , \tag{11}$$

where N_1 and M_1 are, respectively, the axial force and the bending moment in the cross-section of the lower crack arm behind the crack tip. In equations (10) and (11), σ is determined by the Hooke's law (7). Equations obtained after solving the integrals in (10) and (11) for a particular law for distribution of the modulus of elasticity along the beam thickness should be solved with respect to the curvature and the coordinate of the neutral axis.

By substituting of (7), (8) and (9) in (6), one obtains the following expression for the strain energy density in the lower crack arm:

$$u_{01} = \frac{1}{2} E\left(z_1\right)\left[\kappa_1\left(z_1 - z_{1n_1}\right)\right]^2 . \tag{12}$$

Formula (12) is applied also to calculate the strain energy density in the cross-section of the upper crack arm behind the crack tip. For this purpose, z_1 , κ_1 and z_{1n_1} are replaced, respectively, with z_2 , κ_2 and z_{2n_2} where κ_2 and z_{2n_2} are the curvature of the upper crack arm and the coordinate of neutral axis of the upper crack arm. Equilibrium equations (10) and (11) are used to determine z_{2n_2} and κ_2 . For this purpose, N_1 , M_1 , σ , $h_1/2$ and z_1 are replaced, respectively, with N_2 , M_2 , σ_g , $h_2/2$ and z_2 where N_2 and M_2 are the axial force and the bending moment in the cross-section of the upper crack arm behind the crack tip, σ_g is the normal stress in the upper crack arm. The Hooke's law (7) is applied to determine σ_g (the lengthwise strain is obtained by replacing of z_1 , κ_1 and z_{1n_1} with z_2 , κ_2 and z_{2n_2} in formula (9)).

Formula (12) is used also to determine the strain energy density in the beam cross-section ahead of the crack tip by replacing of z_1 , κ_1 and z_{1n_1} , respectively, with z_3 , κ_3 and z_{3n_3} . The curvature, κ_3 , and the coordinate of the neutral axis, z_{3n_3} , of the beam cross-section ahead of the crack tip are obtained after replacing of N_1 , M_1 , σ , $h_1/2$ and z_1 , respectively, with N , M , σ_r , h and z_3 in equilibrium equations (10) and (11). The normal stress, σ_r , in the beam cross-section ahead of the crack tip is found by (7). The distribution of lengthwise strain is determined by (9). For this purpose, z_1 , κ_1 and z_{1n_1} are replaced with z_3 , κ_3 and z_{3n_3} , respectively.

Finally, the strain energy densities in the two crack arms and in the beam cross-section ahead of the crack front are substituted in formula (5) to calculate the strain energy release rate. It should be noted that (5) is applicable for various functionally graded beam configurations, loading conditions and laws for distribution of the modulus of elasticity along the beam thickness. Besides, the lengthwise crack can be located arbitrary along the beam thickness.

3 Numerical Example

This section of the paper presents numerical results obtained by investigating the lengthwise fracture behaviour of a functionally graded cantilever beam configuration by applying the approach for analysis of the strain energy release rate developed in section 2.

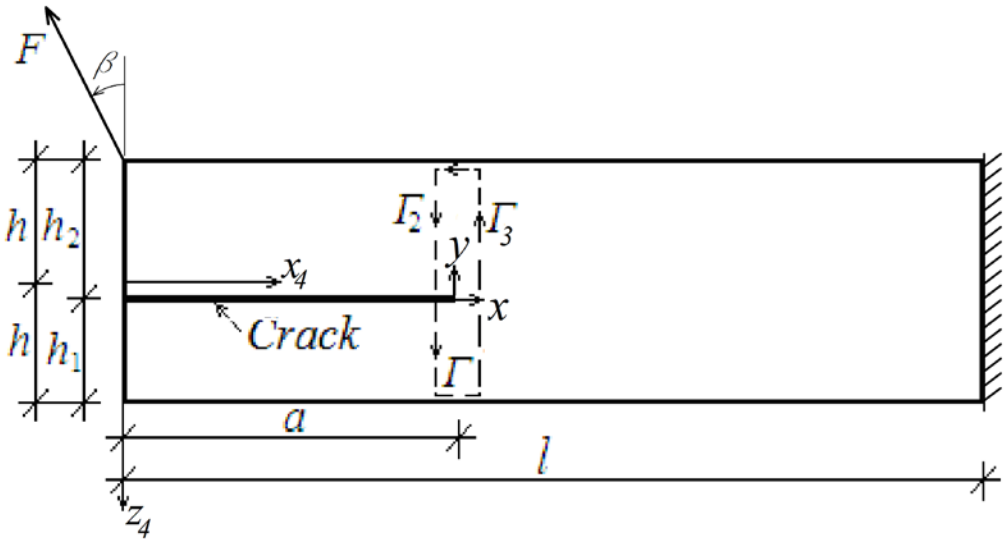

Figure 3. Functionally graded cantilever beam with a lengthwise crack of length, a.

The cantilever beam configuration shown in Figure 3 is considered. A lengthwise crack of length, a, is located arbitrary along the beam thickness. Thus, the two crack arms have different thicknesses denoted by h_1 and h_2. The length of beam is l. The cross-section of beam is a rectangle of width, b, and thickness, $2h$. The beam is clamped in its right-hand end. The beam is loaded by one concentrated force, F, applied at the free end of the upper crack arm (the angle of orientation of F is denoted by β). The lower crack arm is free of stresses. Thus,

$$u_{01} = 0. \tag{13}$$

It is assumed that the modulus of elasticity is distributed continuously along the beam thickness according to the following exponential law:

$$E(z_4) = E_0 e^{s\frac{h+z_4}{2h}}, \tag{14}$$

where

$$-h \le z_4 \le h. \tag{15}$$

Axis, z_4, is shown in Figure 3. In (14), E_0 is the value of modulus of elasticity in the upper surface of the beam, s is a material property that controls the material gradient along the beam thickness.

The fracture behaviour is analyzed in terms of the strain energy release rate by using formula (5). The strain energy density in the cross-section of the upper crack arm behind the crack tip is obtained by applying (12). Equations (10) and (11) are used to determine the curvature and the coordinate of the neutral axis. In order to carry-out the integration in (10) and (11), the modulus of elasticity has to be presented as a function of z_2. For this purpose, (14) is re-written as

$$E(z_2) = E_0 e^{s\frac{z_2+\frac{h_2}{2}}{2h}}, \tag{16}$$

where

$$-h_2/2 \le z_2 \le h_2/2. \tag{17}$$

After replacing of N_1, M_1, σ, $h_1/2$ and z_1 with N_2, M_2, σ_g, $h_2/2$ and z_2, and substituting of (7), (9) and (16) in (10) and (11), one derives the following equations:

$$N_2 = bE_0\kappa_2 e^{\eta}\left\{\frac{1}{\theta^2}\left[e^{\theta\frac{h_2}{2}}\left(\theta\frac{h_2}{2}-1\right)+e^{-\theta\frac{h_2}{2}}\left(\theta\frac{h_2}{2}+1\right)\right]-\frac{z_{2n_2}}{\theta}\left(e^{\theta\frac{h_2}{2}}-e^{-\theta\frac{h_2}{2}}\right)\right\}, \tag{18}$$

$$M_2 = bE_0\kappa_2 e^{\eta}\left\{\frac{1}{\theta^3}\left[e^{\theta\frac{h_2}{2}}\left(\theta^2\frac{h_2^2}{4}-\theta h_2+2\right)-e^{-\theta\frac{h_2}{2}}\left(\theta^2\frac{h_2^2}{4}+\theta h_2+2\right)\right]-\right.$$
$$\left.-\frac{z_{2n_2}}{\theta^2}\left[e^{\theta\frac{h_2}{2}}\left(\theta\frac{h_2}{2}-1\right)+e^{-\theta\frac{h_2}{2}}\left(\theta\frac{h_2}{2}+1\right)\right]\right\}, \tag{19}$$

where $\theta = s/(2h)$, $\eta = sh_2/(4h)$. It follows from Figure 3 that

$$N_2 = F\sin\beta, \tag{20}$$

$$M_2 = Fa\cos\beta - F\frac{h_2}{2}\sin\beta. \tag{21}$$

Equations (18) and (19) are solved with respect to κ_2 and z_{2n_2} by using the MatLab computer program. Then the strain energy density in the upper crack arm is obtained by substituting of (16), z_2, κ_2 and z_{2n_2} in (12).

Equations (18) and (19) are used also to determine κ_3 and z_{3n_3}. For this purpose, M_2, κ_2, h_2 and z_{2n_2} are replaced, respectively, with M_3, κ_3, $2h$ and z_{3n_3} where $M_3 = Fa\cos\beta - Fh\sin\beta$, and then equations (18) and (19) are solved with respect to κ_3 and z_{3n_3}. The strain energy density in the un-cracked beam portion is obtained by substituting of (14), z_3, κ_3 and z_{3n_3} in (12).

By substituting of u_{01}, u_{02} and u_{03} in (5), one derives the following expression for the strain energy release rate in the functionally graded cantilever beam configuration (Figure 3):

$$G = \frac{1}{2}E_0\kappa_2^2 e^{\eta}\left\{\frac{1}{\theta^3}\left[e^{\theta\frac{h_2}{2}}\left(\theta^2\frac{h_2^2}{4}-\theta h_2+2\right)-e^{-\theta\frac{h_2}{2}}\left(\theta^2\frac{h_2^2}{4}+\theta h_2+2\right)\right]-\right.$$

$$-\frac{2z_{2n_2}}{\theta^2}\left[e^{\theta\frac{h_2}{2}}\left(\theta\frac{h_2}{2}-1\right)+e^{-\theta\frac{h_2}{2}}\left(\theta\frac{h_2}{2}+1\right)\right]+\frac{z_{2n_2}^2}{\theta}\left(e^{\theta\frac{h_{22}}{2}}-e^{-\theta\frac{h_2}{2}}\right)\Bigg\}-$$

$$-\frac{1}{2}E_0\kappa_3^2e^{\eta_1}\Bigg\{\frac{1}{\theta^3}\left[e^{\theta h}\left(\theta^2h^2-2\theta h+2\right)-e^{-\theta h}\left(\theta^2h^2+2\theta h+2\right)\right]-$$

$$-\frac{2z_{3n_3}}{\theta^2}\left[e^{\theta h}\left(\theta h-1\right)+e^{-\theta h}\left(\theta h+1\right)\right]+\frac{z_{3n_3}^2}{\theta}\left(e^{\theta h}-e^{-\theta h}\right)\Bigg\}, \tag{22}$$

where $\eta_1 = s/2$.

The solution to the strain energy release rate (22) is verified by applying the *J*-integral method (Broek, 1986). The *J*-integral is solved along the integration contour, Γ, shown in Figure 3. The *J*-integral solution is written as

$$J = J_{\Gamma_2} + J_{\Gamma_3}, \tag{23}$$

where J_{Γ_2} and J_{Γ_3} are, respectively, the *J*-integral values in segments, Γ_2 and Γ_3, of the integration contour (Γ_2 and Γ_3 coincide with cross-sections of the upper crack arm and the un-cracked beam portion, respectively).

The *J*-integral in segment, Γ_2, is written as

$$J_{\Gamma_2} = \int_{\Gamma_2}\left[u_{02}\cos\alpha_{\Gamma_2} - \left(p_{x_{\Gamma_2}}\frac{\partial u}{\partial x} + p_{y_{\Gamma_2}}\frac{\partial v}{\partial x}\right)\right]ds_{\Gamma_2}, \tag{24}$$

where α_{Γ_2} is the angle between the outwards normal vector to the contour of integration in segment, Γ_2, and the crack direction, $p_{x_{\Gamma_2}}$ and $p_{y_{\Gamma_2}}$ are the components of the stress vector, *u* and *v* are the components of the displacement vector with respect to the coordinate system *xy*, and ds_{Γ_2} is a differential element along the contour of integration. The components of (24) are written as

$$p_{x_{\Gamma_2}} = -\sigma_g = -E\varepsilon_g, \tag{25}$$

$$p_{y_{\Gamma_2}} = 0, \tag{26}$$

$$ds_{\Gamma_2} = dz_2 , \tag{27}$$

$$\frac{\partial u}{\partial x} = \varepsilon_g , \tag{28}$$

$$\cos\alpha_{\Gamma_2} = -1. \tag{29}$$

In (25) and (28), the longitudinal strain, ε_g, is determined by replacing of z_1 , κ_1 and z_{1n_1} with z_2 , κ_2 and z_{2n_2} in formula (9) where the coordinate, z_2, varies in the interval $[-h_2/2; h_2/2]$.

By substituting of u_{02}, (25) – (29) in (24), one derives

$$J_{\Gamma_2}=\frac{1}{2}E_0\kappa_2^2e^{\eta}\left\{\ \frac{1}{\theta^3}\left[e^{\theta\frac{h_2}{2}}\left(\theta^2\frac{h_2^2}{4}-\theta h_2+2\right)-e^{-\theta\frac{h_2}{2}}\left(\theta^2\frac{h_2^2}{4}+\theta h_2+2\right)\right]-\right.$$
$$\left.-\frac{2z_{2n_2}}{\theta^2}\left[e^{\theta\frac{h_2}{2}}\left(\theta\frac{h_2}{2}-1\right)+e^{-\theta\frac{h_2}{2}}\left(\theta\frac{h_2}{2}+1\right)\right]+\frac{z_{2n_2}^2}{\theta}\left(e^{\theta\frac{h_{22}}{2}}-e^{-\theta\frac{h_2}{2}}\right)\ \right\}. \tag{30}$$

The solution of the *J*-integral in segment, Γ_3, of the integration contour (Figure 3) is obtained also by (30). For this purpose, h_2 , κ_2 , η and z_{2n_2} are replaced with $2h$, κ_3 , η_1 and z_{3n_3} , respectively. Also, the sign of (30) is set to „minus" because the integration contour is directed upwards in segment, Γ_3.

It should be noted that the *J*-integral solution obtained by substituting of J_{Γ_2} and J_{Γ_3} in (23) is exact match of the solution to the strain energy release rate (22). This fact is a verification of the analysis developed in the present paper.

The solution to the strain energy release rate (22) is verified further by applying the compliance method. According to this method, the strain energy release rate is expressed as

$$G=\frac{F^2}{2b}\frac{dC}{da}, \tag{31}$$

where C is the compliance. For the cantilever beam configuration shown in Figure 3 the compliance is written as

$$C=\frac{w}{F}, \tag{32}$$

where w is the projection of the displacement of the application point of the force, F , on the direction of F . By applying the integrals of Maxwell-Mohr, w is obtained as

$$w=\int_0^a\left(x_4\cos\beta-\frac{h_1}{2}\sin\beta\ \right)\kappa_2(x_4)dx_4+\int_a^l\left(x_4\cos\beta-h\sin\beta\ \right)\kappa_3(x_4)dx_4, \tag{33}$$

where the lengthwise axis, x_4 , is shown in Figure 3. By substituting of (32) and (33) in (31), one derives

$$G=\frac{F}{2b}\left[\left(a\cos\beta-\frac{h_2}{2}\sin\beta\ \right)\kappa_2(a)-\left(a\cos\beta-h\sin\beta\ \right)\kappa_3(a)\right], \tag{34}$$

where κ_2 and κ_3 are determined from equations (18) and (19).

The strain energy release rates obtained by (34) are exact matches of these calculated by (22) which is a conformation for the correctness of the present analysis.

Influence of different factors such as the crack location along the beam thickness, orientatrion of F , material gradient and crack length on the lengthwise fracture behaviour of the functionally graded cantilever beam is evaluated. For this purpose, calculations of the strain energy release rate are performed by applying solution (22). The strain energy release rates obtained are presented in non-dimensional form by using the formula $G_N=G/(E_0b)$. The calculations are carried-out assuming that $F=10$ N, $b=0.005$ m and $l=0.100$ m.

The inluence of the orientation of F on the fracture is investigated. For this purpose, the strain energy release rate is calculated assuming that $0^o \le \beta \le 90^o$. The strain energy release rate is plotted in non-dimensional form against β in Figure 4 at three $2h/b$ ratios. Figure 4 shows that the strain energy release rate decreases with increasing of β. The increase of $2h/b$ ratio leads also to decrease of the strain energy release rate (Figure 4).

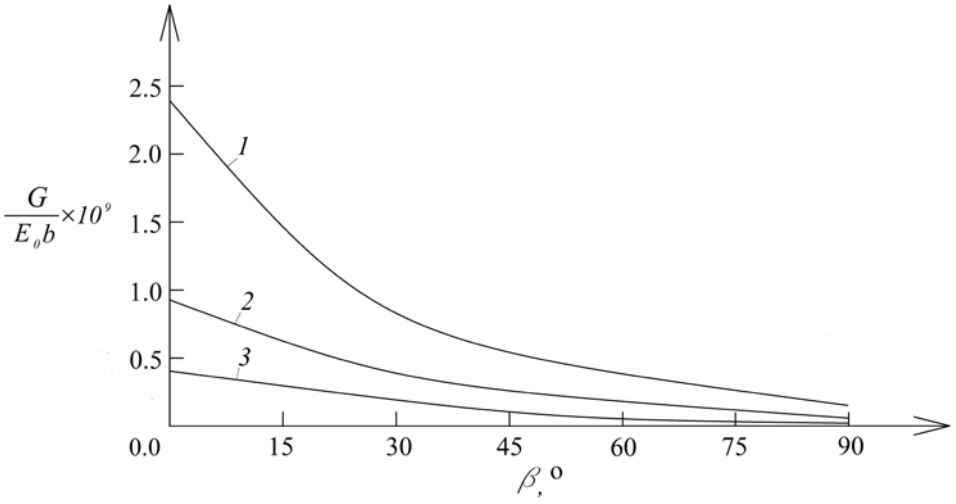

Figure 4. The strain energy release rate in non-dimensional form plotted against β (curve 1 - at $2h/b = 0.6$, curve 2 - at $2h/b = 0.8$ and curve 3 - at $2h/b = 1.0$).

The effects of the crack location along the beam thickness and the crack length on the fracture behaviour are analyzed.

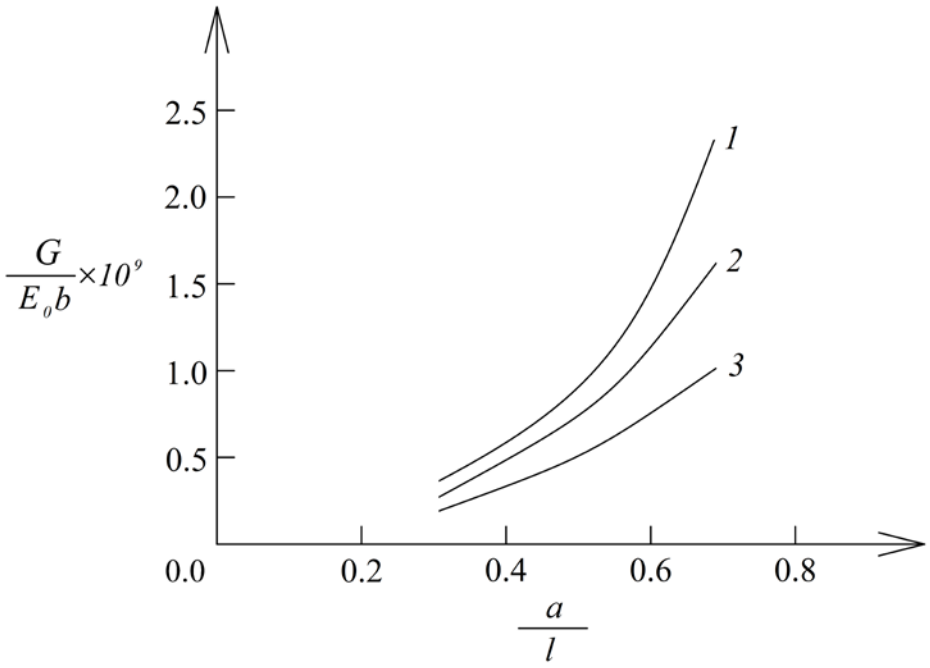

Figure 5. The strain energy release rate in non-dimensional form plotted against a/l ratio (curve 1 - at $h_2/2h = 0.3$, curve 2 - at $h_2/2h = 0.5$ and curve 3 - at $h_2/2h = 0.7$).

The crack location along the beam thickness is characterized by $h_2/2h$ ratio. The ratio, a/l, characterizes the crack length. The strain energy release rate is calculated at three $h_2/2h$ ratios for various a/l ratios. The effects of crack location and the crack thickness on the lengthwise fracture are illustrated in Figure 5 where the

strain energy release rate in non-dimensional form is plotted against a/l ratio at three $h_2/2h$ ratios for $s=0.2$ and $\beta=0$. The curves in Figure 5 indicate that the strain energy release rate increases with increasing of a/l ratio. Concerning the effect of crack location along the beam thickness, Figure 5 shows that the strain energy release rate decreases with increasing $h_2/2h$ ratio (this behaviour is due to the increase of the stiffness of the upper crack arm with increasing of $h_2/2h$ ratio).

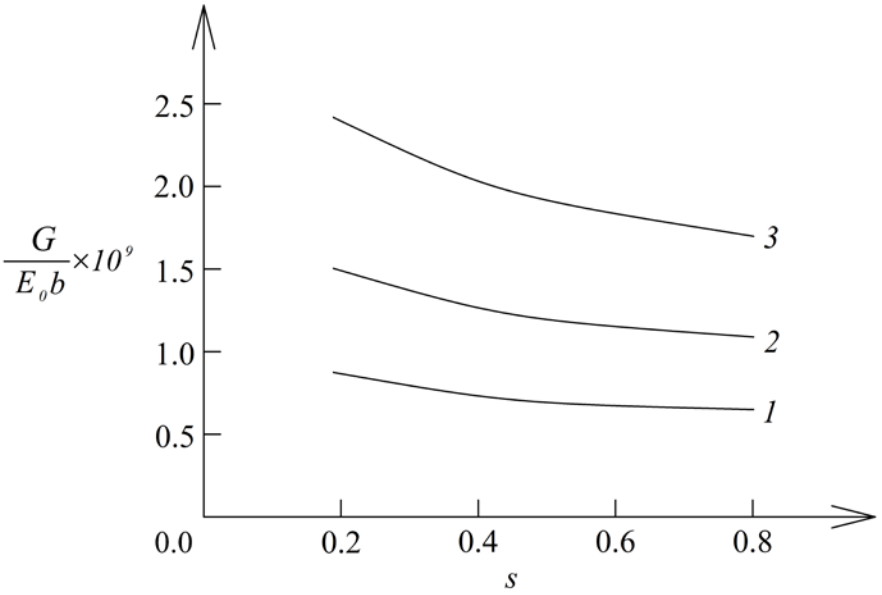

Figure 6. The strain energy release rate in non-dimensional form plotted against s (curve 1 - at $F=6$ N, curve 2 - at $F=8$ N and curve 3 - at $F=10$ N).

The effect of the material gradient along the beam thickness on the fracture is analyzed too. The material gradient is characterized by the parameter, s.

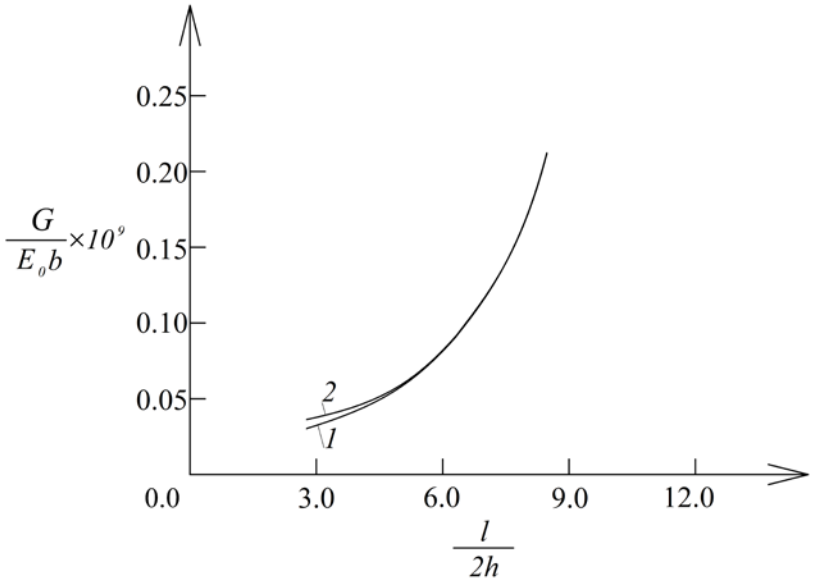

Figure 7. The strain energy release rate in non-dimensional form plotted against $l/2h$ ratio (curve 1 – by applying the classical beam theory, curve 2 – by applying the asymptotically exact beam theory).

The strain energy release rate is calculated at various s for three values of the external force, F. Figure 6 shows the strain energy release rate plotted in non-dimensional form against s at three values of F for

$h_2 / 2h = 0.3$. One can observe in Figure 6 that the strain energy release rate decreases with increasing of s. This behaviour is attributed to the increase of the beam stiffness. The increase of the external force leads also to increase of the strain energy release rate (Figure 6).

The strain energy release rate is calculated also by applying the asymptotically exact beam theory (Le, 2017) and the results obtained are compared with the strain energy release rate derived by solution (22) that is based on the classical beam theory which uses the Bernoulli's hypothesis. The functionally graded linear-elastic cantilever beam configuration shown in Figure 3 is considered. In order to evaluate the effects of the length to thickness ratio of the beam on the lengthwise fracture behaviour, the strain energy release rate calculated by formula (22) and the exact asymptotic beam theory is plotted in non-dimensional form against $l / 2h$ ratio in Figure 7. The curves in Figure 7 indicate that the strain energy release rate increases with increasing of $l / 2h$ ratio. Also, it is evident from Figure 7 that the strain energy release rate derived by using the classical beam theory is in a very good agreement with the results obtained by applying the asymptotically exact beam theory at $l / 2h \geq 5$.

4 Conclusions

A lengthwise fracture in functionally graded beams is analyzed in terms of the strain energy release rate. The beams under consideration are functionally graded in the thickness direction (the modulus of elasticity varies continuously along the beam thickness). It is assumed that the material has linear-elastic behaviour. A general approach for analysis of the strain energy release rate is developed by applying the classical linear-elastic beam theory. The approach is applicable for a crack that is located arbitrary along the beam thickness (the two crack arms have different thicknesses). Thus, the approach can be used to investigate the effect of the crack location on the strain energy release rate for lengthwise cracks in functionally graded beam configurations. Also, the approach is applicable for arbitrary distribution of the modulus of elasticity in the thickness direction of the beam. The strain energy release rate for a lengthwise crack in a functionally graded cantilever beam is analyzed by using the general approach. The cantilever beam is loaded by one force applied at the free end of the upper crack arm. The crack is located arbitrary along the beam thickness. The continuous variation of the modulus of elasticity along the beam thickness is described by applying an exponential law. The *J*-integral approach is used to verify the solution to the strain energy release rate in the cantilever beam. A further check of the solution is carried-out by applying the compliance method. The influence of the crack location along the beam thickness, the orientation of F, the crack length and the material gradient on the strain energy release rate in the cantilever beam is analyzed by using the solution. The calculations show that the strain energy release rate decreaeses with increasing of β. The increase of $2h/b$ ratio leads also to decrease of the strain energy release rate. The analysis reveals that the strain energy release rate decreases with increasing the thickness of the upper crack arm. It is found that increase of the crack length leads to increase of the strain energy release rate. The material gradient in the thickness direction is characterized by the parameter, s. The investigation shows that the strain energy release rate decreases with increasing of s.

Acknowledgments

Rizov gratefully acknowledges the financial support by DAAD for his research stay in Department of Technical Mechanics, Institute of Mechanics, Otto-von-Guericke-University, Magdeburg, Germany.

References

Broek, D.: *Elementary engineering fracture mechanics*. Springer (1986).

Carpinteri, A.; Pugno, N.: Cracks in re-entrant corners in functionally graded materials. *Engineering Fracture Mechanics*, 73, (2006), 1279-1291.

Dolgov, N.A.: Determination of Stresses in a Two-Layer Coating. *Strength of Materials* 37, (2005), 422-431.

Dolgov, N.A.: Analytical Methods to Determine the Stress State in the Substrate–Coating System Under Mechanical Loads. *Strength of Materials* 48, (2016), 658-667.

Erdogan, F.: Fracture mechanics of functionally graded materials. *Comp. Eng.*, 5, (1995), 753-770.

Gasik, M.M.: Functionally graded materials: bulk processing techniques. *International Journal of Materials and Product Technology*, 39, (2010), 20-29.

Jha, D.K.; Kant, T.; Singh, R.K.: A critical review of recent research on functionally graded plates. *Compos. Struct*., 96, (2013), 833–849.

Knoppers, J.W.; Gunnink, J.; den Hout, Van; Van Vliet, W.: *The reality of functionally graded material products*, *TNO Science and Industry*, The Netherlands (2003), 38–43.

Le, K.C.: An asymptotically exact theory of functionally graded piezoelectric shells. *Int. J. Eng. Sci*., 112C, (2017), 42-62.

Mahamood, R.M.; Akinlabi, E.T.: *Functionally Graded Materials*. Springer (2017).

Miyamoto, Y.; Kaysser, W.A.; Rabin, B.H.; Kawasaki, A.; Ford, R.G.: *Functionally Graded Materials: Design, Processing and Applications*. Kluwer Academic Publishers, Dordrecht/London/Boston (1999).

Nemat-Allal, M.M.; Ata, M.H.; Bayoumi, M.R,; Khair-Eldeen, W.: Powder metallurgical fabrication and microstructural investigations of Aluminum/Steel functionally graded material. *Materials Sciences and Applications*, 2, (2011), 1708-1718.

Paulino, G.C.: Fracture in functionally graded materials. *Engng. Fract. Mech*., 69, (2002), 1519-1530.

Rizov, V.: Lengthwise Fracture of Two-Dimensional Functionally Graded Non-Linear Elastic Beam. *Technische Mechanik*, 37, (2017), 48-61.

Rizov, V.: Multilayered Functionally Graded Non-linear Elastic Beams with Logarithmic Material Gradient: A Delamination Analysis. *Technische Mechanik*, 38, (2018), 203-219.

Tilbrook, M.T.; Moon, R.J.; Hoffman, M.: Crack propagation in graded composites. *Composite Science and Technology*, 65, (2005), 201-220.

Upadhyay, A.K.; Simha, K.R.Y.: Equivalent homogeneous variable depth beams for cracked FGM beams; compliance approach. *Int. J. Fract*., 144, (2007), 209-213.

Uslu Uysal, M.; Kremzer, M.: Buckling Behaviour of Short Cylindrical Functionally Gradient Polymeric Materials. *Acta Physica Polonica* A, 127, (2015), 1355-1357, DOI:10.12693/APhysPolA.127.1355.

Uslu Uysal, M.: Buckling behaviours of functionally graded polymeric thin-walled hemispherical shells. *Steel and Composite Structures, An International Journal*, 21, (2016), 849-862.

Uslu Uysal, M.; Güven, U.: A Bonded Plate Having Orthotropic Inclusion in Adhesive Layer under In-Plane Shear Loading. *The Journal of Adhesion*, 92, (2016), 214-235, DOI:10.1080/00218464.2015.1019064.

Wu, X.L., Jiang, P., Chen, L., Zhang, J.F., Yuan, F.P., Zhu, Y.T.: Synergetic strengthening by gradient structure. *Mater. Res. Lett*., 2, 185–191 (2014).

Zhang, Y.; Sun, M.J.; Zhang, D.: Designing functionally graded materials with superior load-bearing properties. *Acta Biomater*, 8, (2011), 1101–1108.

Addresses: Prof. Dr. Victor Rizov, Department of Technical Mechanics, University of Architecture, Civil Engineering and Geodesy, 1 Chr. Smirnensky blvd., 1046 – Sofia, Bulgaria, email: V_RIZOV_FHE@UACG.BG
Prof. Dr.-Ing. habil. Dr.h.c.mult. Holm Altenbach, Lehrstuhl für Technische Mechanik und Geschäftsführender Leiter Institut für Mechanik G10/58, Fakultät für Maschinenbau, Otto-von-Guericke-Universität Magdeburg, Universitätsplatz 2, 39106 Magdeburg, Deutschland, email: holm.altenbach@ovgu.de